

Spill ripple mitigation by bunched beam extraction with high frequency synchrotron motion

S. Sorge,* P. Forck, and R. Singh

*GSI Darmstadt, Planckstraße 1,
64291 Darmstadt, Germany*

(Dated: March 7, 2022)

Abstract

Slow extraction of bunched beams is widely used for mitigating the formation of micro structures due to ripples of the accelerator magnets power supplies on the extracted beam which is also referred to as spill. That helps, in particular, experiments with slow detectors or with low extraction rates. Furthermore, this technique is widely used for avoiding long gaps in the spill measured in ionisation chambers which in turn would trigger interlocks.

On the other hand, the bunches create spill structures on time scales defined by the rf frequency. In addition, macroscopic spill structures of duration up to some hundred milliseconds can be created by the synchrotron motion for a sufficiently large synchrotron tune.

The aim of this report is to study the influence of the synchrotron tune determined by amplitude and harmonic number of the rf voltage which additionally depends on the transverse emittance and the longitudinal bunch area of the circulating beam as well as the distribution of the particles' transit times.

I. INTRODUCTION

Slow extraction from synchrotrons and storage rings is widely used for delivering hadron beams to many fixed target experiments as well as for the irradiation of tumours in hadron cancer therapy. In most cases, a third integer lattice resonance is excited with sextupoles which results in the formation of a triangular area in the phase space plane used for the extraction with stable betatron motion inside, where usually the particles of the whole beam fit in at the beginning of the extraction. The extraction is executed by subsequent feeding the resonance which means that the particles are successively pushed out of that stable phase space area such that their betatron motion becomes unstable, they leave the beam, and become extracted by reaching the extraction septum. The extracted beam is also referred to as spill. Typical extraction time intervals reach from some hundred milliseconds up to hours. Several resonance feeding techniques are presently in operation such as tune sweep, betatron core driven, rf knock-out extraction, where the first two mechanisms are based on the reduction of the size of the stable phase space area, whereas the betatron amplitudes of the particles are slowly increased beyond the edge of the stable phase space area in the

* S.Sorge@gsi.de

last method. The choice of the resonance feeding mechanism depends on the parameters of the beams required by the users such as beam energy and intensity, spill duration, or safety requirements like the ability to suddenly interrupt the extraction if the spill is utilised for the irradiation of patients in medical facilities.

A frequent user requirement to the spill is a low level of undesired temporal structures. Ripples and noise on the current supplied to the accelerator quadrupole magnets could be identified as major source of fluctuations of the machine tune which translate in a ripple of the size of the stable area in the phase space plane and, hence, in structures on the particle flow out of the stable phase space area. These spill micro structures have a characteristic time from ~ 10 ms down to ~ 10 μ s which is too short to be efficiently mitigated by a feedback system [1, 2] and significantly longer than the revolution time.

The particles need after leaving the stable phase space area a certain time T_{tr} for the transit to the extraction septum. These transit times are not uniform and follow a distribution instead. The width of the distribution defines a transit time spread ΔT_{tr} . Thereby, temporal structures formed by particles which left the stable phase space area at the same instant are smeared out. That mechanism can be utilised for reduction, especially, of spill micro structures while applying an extraction technique which does not rely on longitudinal dynamics as for example slow extraction of unbunched beam by tune sweep. On the other hand, spill micro structures can be mitigated with help of longitudinal dynamics, where the basic mechanism consists in the change of the momenta and, thus, the chromatic tunes of particles towards the resonance tune by rf fields which results in a transition across the edge of the stable phase space area much faster than that caused by the resonance feeding. Thereby, the duration of stay of particles near the separatrix is reduced and the level of structures imprinted on the particle flux out of the stable phase space area is reduced. The particle momenta can be quickly changed by applying rf fields of defined harmonic number resulting in synchrotron motion during slow extraction of bunched beams or channelling between empty rf buckets, or by driving longitudinal diffusion by rf noise with a band limited power spectrum during stochastic extraction. The aim of the present report is to study mitigation and also formation of spill structures during slow extraction of bunched ion beams out of the present heavy ion synchrotron SIS18 of the GSI facility within a simulation study for synchrotron motion significantly faster than usually applied in present operation. Hence, the work is restricted to slow extraction by tune sweep performed with two fast

ramped quadrupoles which is the standard slow extraction technique of SIS18. That topic is motivated by the plan to install a special high frequency rf cavity in order to provide rf fields with a harmonic number increased by an order of magnitude which is required by an experiment collaboration with the goal to take advantage of spill micro structure reduction provided by bunched beam extraction and to avoid spill structures at typical present rf frequencies. That requirement implies a strongly increased synchrotron tune.

Generally, the results of the study show that a gain in spill quality by increasing the synchrotron tune and according reduction of the duration of stay of the particles near the oscillating edge of the stable phase space area can be achieved only up to an optimum of the synchrotron tune, whereas further rise reduces the spill quality. Reasons are that the transit time distribution during bunched beam slow extraction has a reduced but still significant influence on the spill quality and, in addition, is itself modified by the synchrotron motion. Furthermore, the creation of macroscopic spill structures is found for a sufficiently large synchrotron tune. The conditions resulting in such phenomena are analysed and possible ways of mitigation are proposed.

II. CONDITIONS FOR SLOW EXTRACTION FROM SIS18 ASSUMED IN THE STUDY

The present study is focused on the present GSI heavy ion synchrotron SIS18, but the results are applicable to other machines like SIS100 or hadron therapy synchrotrons.

As in most synchrotrons, slow extraction from SIS18 is based on the excitation of a one-dimensional third integer resonance with sextupoles resulting in the formation of a triangular area of stable betatron motion in the phase space plane used for the extraction which is the horizontal phase plane in SIS18. The stable phase space area formation can be described by the Kobayashi theory [3]. The size of the stable phase space area is given by its corners which are unstable fixed points (UFP) of betatron motion. Written in normalised coordinates of the phase space vector $\vec{X} = (X, X')$ with

$$X \equiv \frac{x}{\sqrt{\beta_x}} \text{ and } X' \equiv \sqrt{\beta_x}x' + \frac{\alpha_x}{\sqrt{\beta_x}}x, \quad (1)$$

the UFPs have all the same absolute value [4]

$$\left| \vec{X}_{\text{UFP}} \right| = 8\pi \left| \frac{Q_r - Q_p}{S_v} \right|, \quad (2)$$

where Q_r and Q_p are resonance tune and on axis tune of the particles. The latter can be modified by chromaticity ξ and relative momentum deviation δ of the particles to

$$Q_p = Q_m + \xi\delta. \quad (3)$$

S_v in Equation (2) is the strength of a virtual sextupole and given by

$$S_v \cdot e^{3i\psi_v} = \sum_n S_n e^{3i\psi_n} \quad (4)$$

with the normalised sextupole strength of the n th sextupole

$$S_n = \frac{1}{2} \beta_{x,n}^{3/2} (k_2 L)_n \quad (5)$$

and the betatron phase advance ψ_n between the location of the n th sextupole and the considered location which is usually the entrance of the electro-static septum. The ψ_n have to be determined for the third integer tune of the resonance Q_r . The resulting area of the stable phase space area is

$$A_{\text{stable}} = 3 \frac{1}{2} |\vec{X}_{\text{UFP}}|^2 \sin 120^\circ = \frac{\sqrt{27}}{4} |\vec{X}_{\text{UFP}}|^2. \quad (6)$$

The corresponding emittance is

$$\epsilon_{\text{stable}} = \frac{A_{\text{stable}}}{\pi}. \quad (7)$$

The dependence of A_{stable} on the tune can be used for extracting the beam by moving the machine tune Q_m slowly across the resonance tune by changing the focusing strengths of quadrupoles such that it shrinks and the particle become successively unstable according to their transverse emittance and momentum dependent tune such that they leave the synchrotron. This technique referred to as quadrupole driven extraction is the present standard technique for slow extraction from SIS18. Hence, this manuscript is focused on the usage of this method.

A very comprehensive series of machine experiments was performed with beams of Ar^{18+} ion at the beam energy $E = 500 \text{ MeV/u}$. Typical particle numbers were between 10^5 and 10^6 ions per cycle which is lower than in user experiments. The purpose was to use a scintillation counter for measuring the spill which has a limited count rate. But it allows for experiments with a high time resolution which was actually chosen to $10 \mu\text{s}$. In addition, it provides the opportunity to perform particle tracking simulations with particle numbers

similar to those of the measurements. These experiments delivered the most important results the particle tracking results achieved in this study are compared with. For that reason, we apply conditions in the simulation of the present study similar to those in these experiments.

III. SPILL SIMULATIONS AND CHARACTERISATION OF SPILL MICRO STRUCTURES

Spill structures can be investigated by simulating the process of slow extraction with particle tracking. We use the MAD-X code for the simulations. Gaussian distribution functions truncated at 2σ are applied to set the initial coordinates of the test particles. 10^5 particles were tracked in each simulation for $5 \cdot 10^5$ revolutions after finishing the bunching process. The σ values of corresponding Gaussian distribution functions of the transverse particle coordinates are defined by the rms beam emittances $\epsilon_{x,\text{rms}} = 3.9$ mm mrad and $\epsilon_{y,\text{rms}} = 1.3$ mm mrad. The resulting maximum beam emittances are $\epsilon_{x,\text{max}} = 15.5$ mm mrad and $\epsilon_{y,\text{max}} = 5.2$ mm mrad, respectively. They arise from the beam width given by the machine acceptance during injection and subsequent adiabatic shrinkage during acceleration. In order to study the influence of the horizontal beam width, transverse beam emittances reduced by the factor 0.2 are applied. The maximum momentum deviations δ_m reach from $\delta_m = 5 \cdot 10^{-4}$ up to $\delta_m = 10^{-3}$, where the actual value depends on the rf voltage defined by amplitude V_{rf} and harmonic number h .

The time resolution for measuring spills is given by the measurement rate of the spill measurement system, where $f_{\text{sample}} = 100$ kHz in SIS18. The resulting upper limit to the frequency range of the spill micro structures is then $f_{\text{up}} = f_{\text{sample}}/2 = 50$ kHz.

The quantity used for characterising the spill quality defined by the micro structure level in this study is the time dependent duty factor [5]

$$F(t) = \frac{\langle N \rangle^2(t)}{\langle N^2 \rangle(t)} = \frac{N_{\text{av}}^2(t)}{N_{\text{av}}^2(t) + \sigma_N^2(t)} \quad (8)$$

is applied, where $\langle x \rangle$ denotes the average of the variable x given in time intervals according to the measurement resolution $t_{\text{meas}} = 1/f_{\text{meas}}$ in time intervals t_{rec} which define the average length. The latter defines the recording resolution. The actual size of the measurement and recording time intervals used for this study were $t_{\text{meas}} = 10 \mu\text{s}$ and $t_{\text{rec}} = 10$ ms. A good

spill quality given by a low spill structure level results in large value of the time dependent duty factor.

The upper limit to $F(t)$ under realistic beam conditions and for $t_{\text{rec}} \gg t_{\text{meas}}$ is reached in the Poisson limit which denotes stochastic distribution of extracted particles in the time intervals. For Poisson's distribution function to find N particles in a measurement time interval,

$$f_P = e^{-\lambda} \frac{\lambda^N}{N!} \quad (9)$$

one finds $N_{\text{av}}^2 + \sigma_N^2 = (N^2)_{\text{av}} = N_{\text{av}} (N_{\text{av}} + 1)$ such that

$$F_P(t) = \frac{N_{\text{av}}(t)}{N_{\text{av}}(t) + 1}. \quad (10)$$

It can be useful to reduce the time dependent duty factor to the weighted factor defined in [6] by

$$\begin{aligned} F_{\text{av}} &= \frac{\int dt \dot{N}(t) F(t)}{\int dt \dot{N}(t)} \\ &= \frac{\sum_k N_k F_k}{\sum_k N_k} \end{aligned} \quad (11)$$

which is, basically, the time average of the weight function $\dot{N}(t)$ which is the extraction rate at instant t denoting the spill. On the other hand, spill and time dependent duty factor are recorded with the time resolution given by t_{rec} such that, approximately, $N_k = \dot{N}(t_k) \cdot t_{\text{rec}}$ with $t_k = k \cdot t_{\text{rec}}$ and the integrals represented by the sums in the second row of Equation (11).

IV. MITIGATION OF SPILL MICRO STRUCTURES WITH BUNCHING

The spread of the particles' transit times ΔT_{tr} arising from the width of the transit time distribution results in a finite interval of arrival times of particles which became unstable at the same instant. Hence, spill micro structures imprinted by oscillations of the stable phase space area's size due to a tune ripple are smeared out. This mechanism could be identified as a major spill smoothing mechanism for slow extraction of coasting beams [6, 7].

In contrast to the aforementioned mechanism, spill smoothing for bunched beam slow extraction is mainly based on the periodic change of the particles' tune due to synchrotron

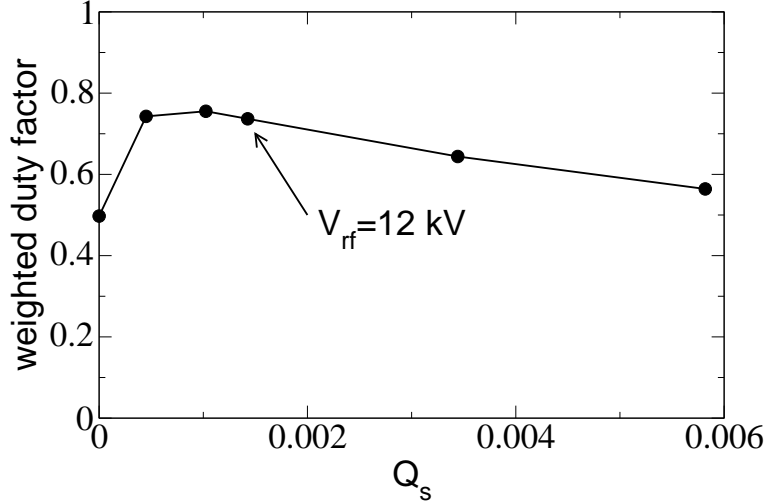


FIG. 1. Weighted duty factors according to Equation (11) of spills obtained in simulations of the slow extraction of Ar^{18+} beams from SIS18 at the beam energy $E = 500$ MeV/u as function of the synchrotron tune according to the the rf voltages $V_{\text{rf}} = (0, 1.2, 6.2, 12, 70, 200)$ kV, where $V_{\text{rf}} = 12$ kV is the maximum which can be reached in SIS18. The rf voltage at the beginning of the simulations is switched off and slowly turned on during the first 50000 turns. The initial maximum momentum width is $\delta_m = 5 \cdot 10^{-4}$ and is increased during the bunching process. Hence, also longitudinal dynamics with low rf voltages with particles captured and others not captured in the rf bucket are well described.

motion which yields a transition from stable to unstable betatron motion significantly faster than caused by the tune sweep. Therefore, the particles will stay much shorter near the oscillating edge of the stable phase space area such that resulting structures imprinted on the spill are strongly reduced. Following this reasoning, one would expect that the spill quality defining duty factor always grows for an increasing synchrotron tune Q_s or, at least, saturates because the time the particles are near the separatrix can not be reduced below zero. However, it is found by performing particle tracking simulations of the extraction that the weighted duty factor has a maximum at a certain Q_s and is decreased if Q_s is further increased which one can see in Figure 1. Our analysis reveals that particles are re-captured into the stable phase space area after becoming unstable if the synchrotron motion is too fast such that they can not become extracted. As a result, the distribution of the transit times of extracted particles is altered. That suggests that the influence of the transit time distribution is only reduced but not irrelevant.

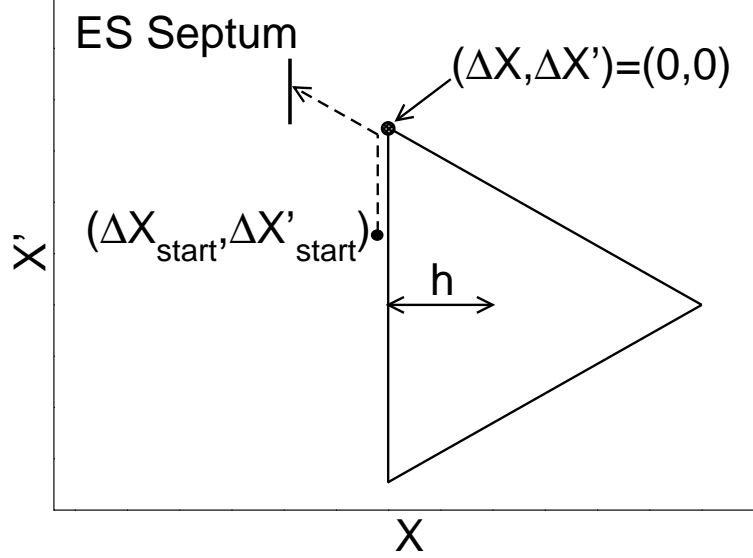


FIG. 2. Schematic representation of the stable phase area in normalised coordinates X, X' defined relative to the centre of the triangle. The starting coordinates $\Delta X_{\text{start}}, \Delta X'_{\text{start}}$ relevant for the time of a particle's transit from the stable phase area to the electro-static septum are defined relative to the upper left corner of the triangle.

We apply a model based on the analytic expression for the transit time from Equation (4.13) in [8]

$$T_{\text{tr}} \approx \frac{1}{\sqrt{3}\varepsilon} \ln \left| \frac{1}{1 - \Lambda_0^2} \frac{n}{n + 3} \frac{3}{\lambda_0} \right|, \quad (12)$$

in order to demonstrate the effect of the synchrotron motion on the transit time distribution. The variables in this equation are $\varepsilon = 6\pi|Q_{x,r} - Q_x(\delta)|$, $\lambda_0 \equiv -\Delta X_{\text{start}}/h$ and $\Lambda_0 \equiv -\Delta X'_{\text{start}}/(2\sqrt{3}h)$ with the coordinates of the start of a particle's transition in horizontal phase space $\Delta X_{\text{start}}, \Delta X'_{\text{start}}$, and $n \equiv -\Delta X_{\text{ESS}}/h$. One should note that $\Delta X_{\text{start}}, \Delta X'_{\text{start}}$, and the normalised horizontal coordinate of the electro-static septum ΔX_{ESS} are defined relative to the point $(\Delta X, \Delta X') = (0, 0)$ at the upper left corner of the triangular stable phase space area shown in Figure 2 and, hence, negative. The transit time in this formula is dimensionless and given in units of three subsequent revolutions. By applying the analytic formula, the effect can be directly depicted. That is an advantage compared to the use of simulation data, where it is difficult to determine the instant when a particle becomes unstable and its transit from the stable phase area to the extraction septum begins.

From Equation (12), it follows that the transit time of a particle is the shorter the larger λ_0 is, where a large value of λ_0 corresponds to a large distance of a particle's starting point

ΔX_{start} from the separatrix. The maximum distance ΔX_{start} during a synchrotron period is reached at the cusp of synchrotron motion, where the momentum dependent tune

$$Q(\delta) = Q_m + \Delta Q(\delta) \text{ with } \Delta Q(\delta) = \xi \delta \quad (13)$$

is closest to the resonance tune Q_r . On the other hand, the chromatic tune of particle will move away from the resonance after it has passed the cusp and after a certain time it will re-enter the stable phase space area if it has not reached the extraction septum, yet. This limiting time t_{lim} can approximately be defined by

$$t_{\text{lim}} = T_s \frac{\psi_s}{2\pi}, \quad (14)$$

where ψ_s is the synchrotron phase angle shown in Figure 3. The ellipse in this figure represents the trajectory in longitudinal phase space with the largest synchrotron amplitude which corresponds to the maximum ψ_s . ψ_s will be the smaller the less the cusp of the trajectory goes beyond the stability frontier at the instant $t + T_s$. In addition, particles with a short t_{lim} will start their transit from only a little outside the stable phase space area at $t + T_s$. Hence, ΔX_{start} and λ_0 of such particles in Equation (12) is small and will result in a long transit time. In other words, longer transit times T_{tr} will be suppressed by shorter limiting times t_{lim} .

In order to demonstrate the effect, the transit time distribution will be determined in two steps for conditions of an Ar^{18+} beam at the beam energy $E = 500 \text{ MeV/u}$. The two rf voltages $V_{\text{rf}} = 6.2 \text{ kV}$ and $V_{\text{rf}} = 12.0 \text{ kV}$ are applied which are the largest used in the measurements. Further simplifying assumptions are:

1. the distribution of the momentum deviations δ is symmetric with respect to the sign of δ and the maximum for all cases is $\delta_m = 0.0005$,
2. the synchrotron tune does not depend on the synchrotron amplitude and is given by [9]

$$Q_s = \sqrt{\frac{ZehV_{\text{rf}}|\eta \cos \phi_s|}{2\pi\beta^2 E_{\text{tot}}}} \quad (15)$$

with the charge of the ions Ze , harmonic number and amplitude of the rf voltage h , V_{rf} , the phase slip factor η , the phase of the synchronous particle ϕ_s , the relativistic factor $\beta = v/c$, and the total energy of an ion $E_{\text{tot}} = Am_{\text{u}}c^2\gamma$ with the number of nucleons in the ion's nucleus, $m_{\text{u}}c^2 = 931.494 \text{ MeV}$ and $\gamma = 1/\sqrt{1 - \beta^2}$.

3. the particle density does not depend on betatron and synchrotron coordinates.

In the first step, the transit time distribution is determined according to the initial particles $\Delta X_{\text{start}}, \Delta X'_{\text{start}}$ as well as the momentum dependent difference between particle and resonance tunes but neglecting the limitation of the transit times due to the synchrotron motion. The resulting transit time distributions are shown in Figure 5. They appear rather independent from the synchrotron tune.

In the second step, the limitation of the transit times due to the synchrotron motion is taken into account. It turns out that, after a single synchrotron period, none of the particles is extracted for all considered rf voltages. For that reason, the machine tune is further moved towards the resonance in time steps of the synchrotron period. In addition, we assume that the betatron amplitude of the particles has not changed during the short stay outside the stable phase space area such that the horizontal start coordinates relative to the centre of the stable phase area, $X_{\text{start}}, X'_{\text{start}}$ are not changed. The distance of the starting point from the separatrix, ΔX_{start} and, hence, λ_0 , of all particles will increase because of the shrinking stable phase area denoted by a decreasing $h(t)$ in the transit time formula above. That will result in a decrease of the transit times T_{tr} such that they will become shorter than the limiting times t_{lim} . The resulting in the transit time distributions are those of the particles which reach the extraction septum. They are shown in Figure 6. The corresponding averaged transit times and rms spreads are

$$V_{\text{rf}} = 6.2 \text{ kV} : T_{\text{tr,av}} = 162 \text{ rev.}, \Delta T_{\text{tr,rms}} = 44 \text{ rev.}$$

$$V_{\text{rf}} = 12.0 \text{ kV} : T_{\text{tr,av}} = 116 \text{ rev.}, \Delta T_{\text{tr,rms}} = 33 \text{ rev.}$$

The results suggest that the decrease of the transit time spread for the rf voltage increased from 6.2 kV to 12 kV which results in the decrease of the duty factor has a **stronger** impact than the decrease of the stay of the particles near the oscillating edge of the horizontal stable phase space which would result in a reduced spill micro structure level.

One should note that the differences of the mean and rms values of the transit times found for the considered rf voltages are rather underestimated because the increase of the synchrotron period for increased synchrotron amplitude is neglected which rather occurs for lower voltages.

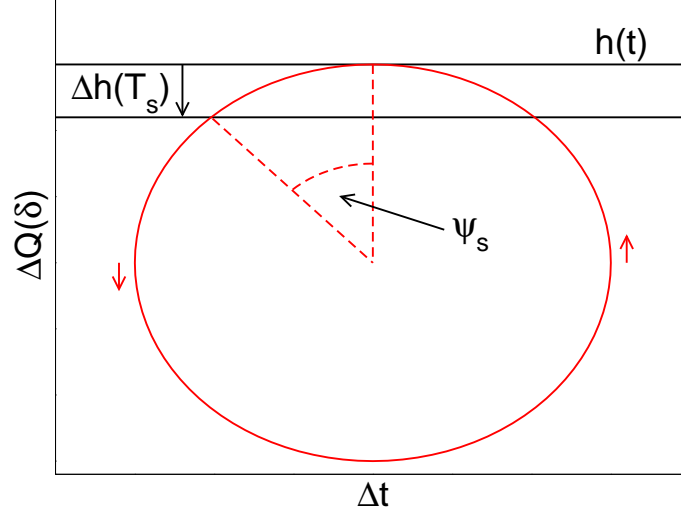


FIG. 3. Range of longitudinal coordinates of particles with certain horizontal emittance related to the size of the stable phase space area characterised by $h(t)$ at instant t and shrunk within a synchrotron period T_s by $\Delta h(T_s)$.

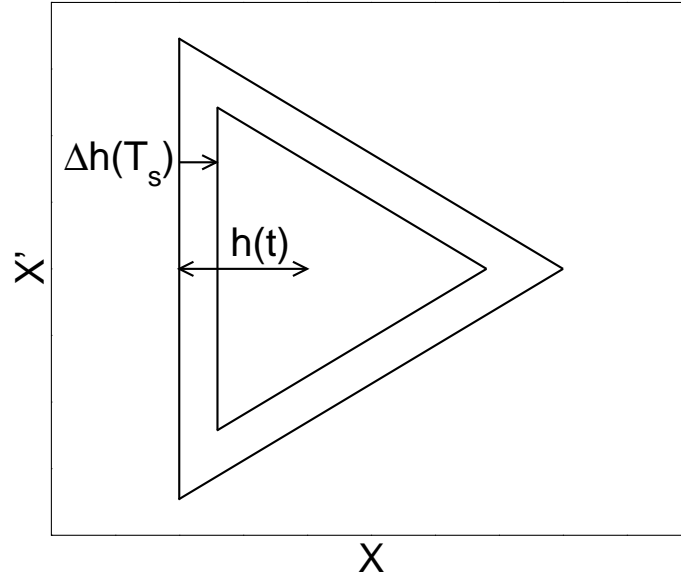


FIG. 4. Schematic plot of the stable phase space area at instant t and shrunk within a synchrotron period by moving the machine tune $Q_{x,m}$ towards the resonance tune $Q_{x,r}$.

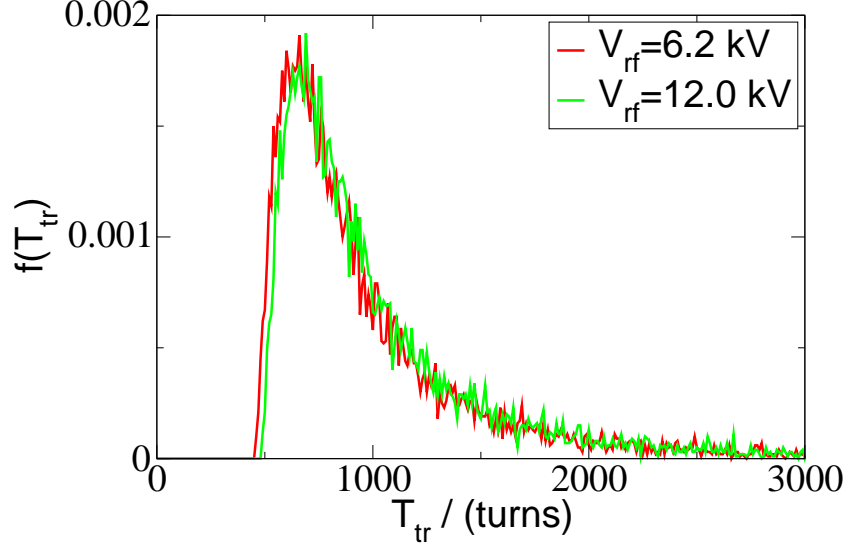


FIG. 5. Distributions of the transit times according to Equation (12) without taking into account the limitation arising from the re-capture of particles into the stable phase area due to synchrotron motion for the same conditions as those for Figure 1.

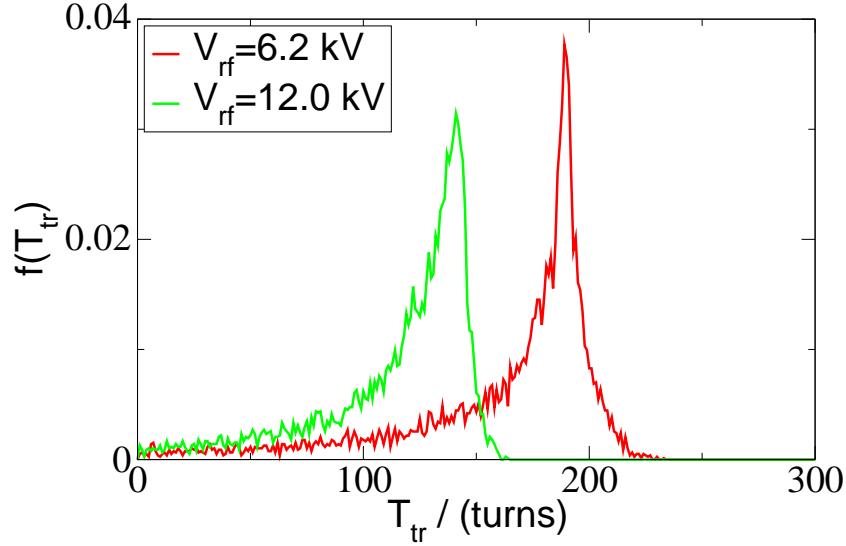


FIG. 6. Distributions of the transit times as determined in Figure 5, where the limitation is taken into account which arises from the re-capture of particles into the stable phase area due to synchrotron motion. Hence, the distributions in this figure represent the real transit times of the particles which reach the extraction septum.

V. SPILL NANO STRUCTURES

The improvement of the spill quality on microscopic time scales due to bunching occurs at the price of the creation of spill structures on time scales defined by the rf frequency

$$f_{\text{rf}} = f_{\text{rev}} \cdot h \quad (16)$$

with the revolution time f_{rev} and the harmonic number of the rf fields h . The rf frequency of the present SIS18 rf cavity reaches up to $f_{\text{rf}} = 6$ MHz [10]. According to a typical revolution time $t_{\text{rev}} \in [0.8, 1.0] \mu\text{s}$ during extraction, the rf harmonic number is usually $h = 4$ or $h = 5$ and the total duration of an rf bucket is $t_{\text{bucket}} \in [200, 250]$ ns. Hence, these structures are referred to as spill nano structures.

The length of the bunches in the extracted beam is found to be shorter than that in the circulating beam [11]. The reason is that only particles are extracted which are near the cusp of synchrotron motion such that their chromatic tune reaches the phase space range of unstable betatron motion which is, basically, the area in the longitudinal trajectory marked by the red ellipse in Figure 3 and the black solid lines which mark the frontier between stable and unstable motion at beginning and ending of a synchrotron period. In addition, most particles will start with their transit towards the extraction channel after they have passed the cusp of synchrotron motion because the transit time reaches its minimum there which is pointed out in Section IV.

An example for resulting profiles of circulating and extracted bunches as function of the arrival time compared to that of the synchronous particle obtained from simulation data are shown in Figure 7. The length given by the full length at half maximum intensity of the circulating bunch under the chosen conditions is about $t_{\text{b,circ}} = 84$ ns, whereas that of the extracted bunch integrated over the whole extraction process is $t_{\text{b,ex}} = 40$ ns. The full bucket length is $t_{\text{bucket}} = 190$ ns such that the duration of the void between two bunches is $t_{\text{void,circ}} = 106$ ns for the circulating beam and even $t_{\text{void,ex}} = 150$ ns for the extracted beam. In addition, one should keep in mind that the extracted bunch in Figure 7 is averaged over the whole extraction such that it is longer than an instantaneous bunch. As a result, the intensity of the beam arriving at the target will have a **strong** variability. That limits the maximum intensity and, hence, the event rate of some experiments because the integration time of the detector is comparable or shorter than the duration of a bunch. E. g. the HADES detector has an integration time of $t_{\text{int}} = 140$ ns. For that reason, the number

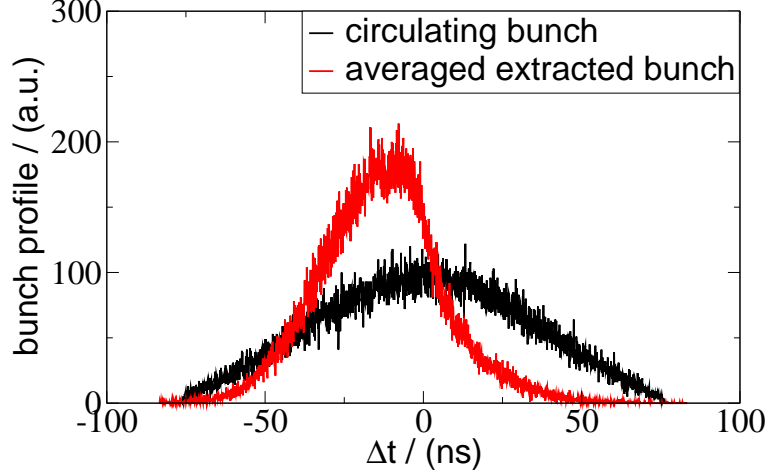


FIG. 7. Intensity profiles as function of the time difference to the synchronous particle of a circulating bunch and the resulting extracted bunches averaged over the time of the whole extraction process obtained in a simulation for conditions used in Figure 1 with $h = 5$ and $V_{rf} = 6.2$ kV.

of particles detected in an integration time will be given by the maximum intensity which can lead to a pile up in case of a too large averaged intensity or it will be zero when a void is detected which means waste of detection capacity [12, 13]. A possible solution is to increase the rf frequency to at least $f_{rf} \geq 40$ MHz. Actually, the installation of an rf cavity with a frequency $f_{rf} = 80$ MHz is planned such that the duration of an rf bucket would shrink to $t_{bucket} = 12.5$ ns and always five or six bunches arrive within an integration time at the detector [14]. The result would be a much lower fluctuation level of particles detected in subsequent detector integration times. The generation of bunches with such a high rf frequency results in **fast** synchrotron motion because $Q_s \propto \sqrt{h}$.

VI. MACROSCOPIC SPILL STRUCTURES ARISING FROM FAST SYNCHROTRON MOTION

It is shown in Section IV that there is an optimum of the synchrotron tune above which the level of spill micro structures is again increased for further increased Q_s . An additional limitation to the improvement of the spill quality found in our studies is that synchrotron motion with sufficiently large synchrotron tune can result in the formation of macroscopic spill structures of duration ~ 0.1 s or longer. Such structures could be found for conditions of present SIS18 operation in measurements as well as in simulations, see Figures 8 and 9.

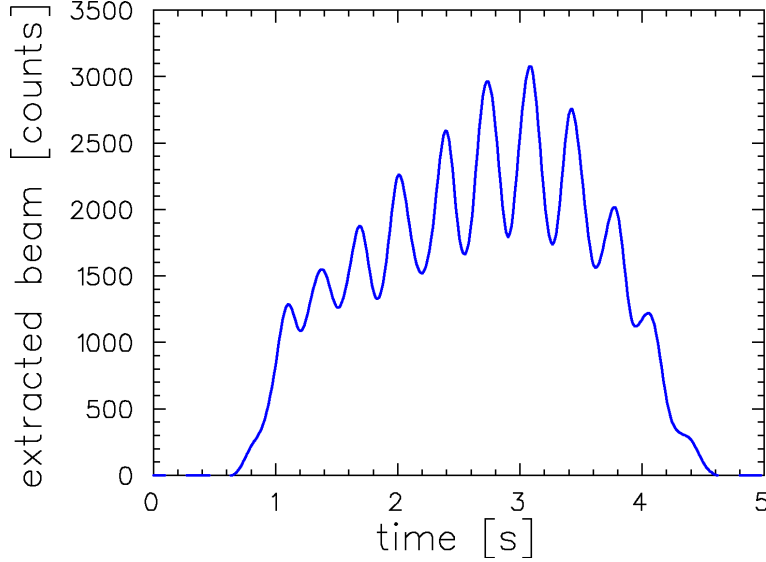


FIG. 8. Spill of an Ar^{18+} beam measured during slow extraction from SIS18 at the beam energy $E = 500$ MeV/u bunched with the rf voltage of amplitude $V_{\text{rf}} = 12$ kV and harmonic number $h = 5$.

These figures show spills of the extraction Ar^{18+} beams at beam energy $E = 500$ MeV/u bunched with an rf voltage of amplitude $V_{\text{rf}} = 12$ kV and harmonic number $h = 5$. Crossing synchro-betatron coupling resonances could be identified in tracking simulations as a likely mechanism. These resonances are defined by the condition [15]

$$kQ_x + lQ_y + mQ_s = n, \quad (17)$$

where k, l, m, n are integer numbers, where $k = 3$, $l = 0$, and $n = 3 \cdot Q_{x,r} = 13$. In simulations, the exact time behaviour of Q_x is known and, hence, it can be detected when such a resonance is crossed. In doing so, a clear correlation between the instants when Q_x is fulfilling the resonance condition and the appearance of the structures could be found which one can see in Figure 9. That figure makes also visible that quadrupole ripples inhibit the formation of macroscopic structures, where the spill obtained with the quadrupole ripple of amplitude zero resembles more the measured spill in Figure 8.

The macroscopic structures are found to depend on the rf voltage, the horizontal beam emittance, and the momentum width, where the macroscopic spill structures become more visible for a higher rf voltage because the distance between the resulting synchro-betatron resonances is larger such that they can be better resolved. In addition, the structures shown in Figure 9 are found for bunches with a maximum momentum deviation $\delta_{\text{max}} = 5 \cdot 10^{-4}$

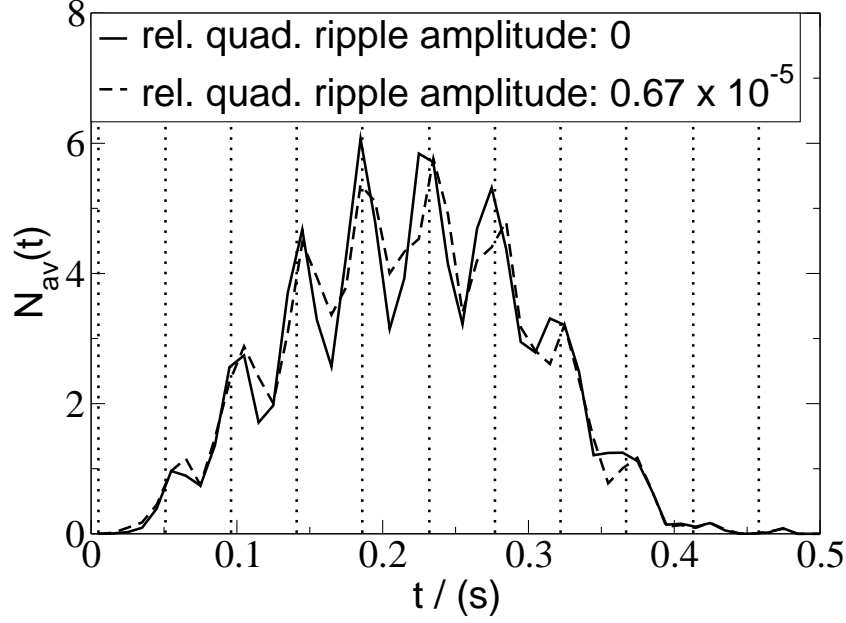


FIG. 9. Spill of an Ar^{18+} beam obtained in a slow extraction simulation for SIS18 conditions at the beam energy $E = 500$ MeV/u, where $V_{\text{rf}} = 12$ kV, $h = 5$, and quadrupole ripples of two different amplitudes are applied. The transverse beam emittances correspond to the machine acceptance at injection reduced by the factor 0.2 and adiabatic shrinkage during acceleration afterwards. Furthermore, the maximum momentum deviation in the bunches is $\delta_m = 5 \cdot 10^{-4}$. Both, the transverse emittances and the maximum momentum deviation are lower than during usual SIS-18 operation. The dotted vertical lines mark the moments when the machine tune crosses a synchro-betatron resonance. The third integer resonance corresponding to $m = 0$ in Equation (17) is crossed at $t = 0.41$ s.

and a horizontal beam emittance $\varepsilon_x = 3.1$ mm mrad. The latter is achieved by filling the total machine acceptance at injection to 20 % and subsequent adiabatic shrinkage during acceleration. Both values are lower than during regular SIS18 operation. The structures are diminished or even vanish if the horizontal emittance or the momentum width is increased. It turns out that the horizontal emittance has a **stronger** influence than the momentum width which is demonstrated by repeating the simulations with increased momentum width and horizontal emittance, respectively. The resulting spills are shown in Figure 10. They suggest that macroscopic spill structures should not play an important role in present SIS18 operation.

The situation will be different if the harmonic number of the rf field h is increased by

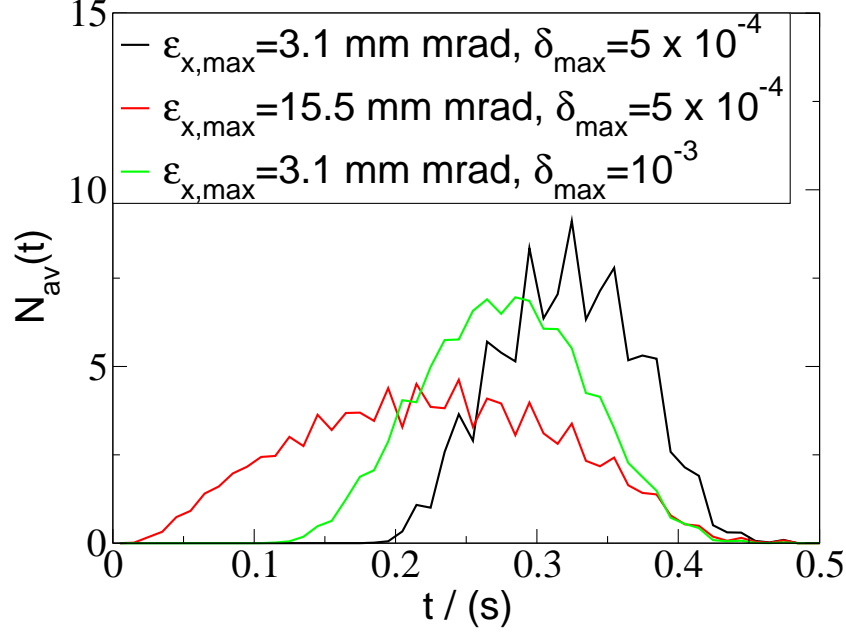


FIG. 10. Spills obtained for Ar^{18+} beam at beam energy $E = 500$ MeV/u bunched with the rf voltage of harmonic number $h = 5$ and amplitude $V_{\text{rf}} = 12$ kV with varied horizontal emittance and momentum width. The black curve corresponds to the solid black curve in Figure 9, where the initial horizontal tune is changed from $Q_{x,\text{ini}} = 4.329$ in the figure above to $Q_{x,\text{ini}} = 4.327$ in this figure in order to enable the application of increased horizontal emittance and momentum width.

a factor of about 20 which will result in a **strongly** increased synchrotron tune. That is demonstrated in the following by examining the example of an Ar^{18+} beam extracted at the same energy as in the example above but the harmonic number increased to $h = 100$. In the first step, the rf voltage amplitude to $V_{\text{rf}} = 70$ kV is assumed which is planned to be the maximum of the high frequency cavity foreseen to be installed in SIS18 [14]. The resulting spill obtained by particle tracking is shown in Figure 11. The horizontal tune in this example is shifted from $Q_{x,i} = 4.326$ to $Q_{x,f} = 4.334$. The synchrotron tune is $Q_s = 0.015$ such that the gap between two synchro-betatron resonances is a little lower than three times the horizontal tune interval crossed during the extraction, $\Delta Q_x = 0.024$. Two resonance are crossed which are marked by the dotted lines in Figure 11, where the horizontal third integer resonance is that crossed at $t = 0.48$ s. In addition, this figure shows that the extraction rate has its maximum near the resonance crossed first at $t = 0.18$ s. The reason is that the number of particles in the beam when reaching the third integer resonance is already **strongly** reduced.

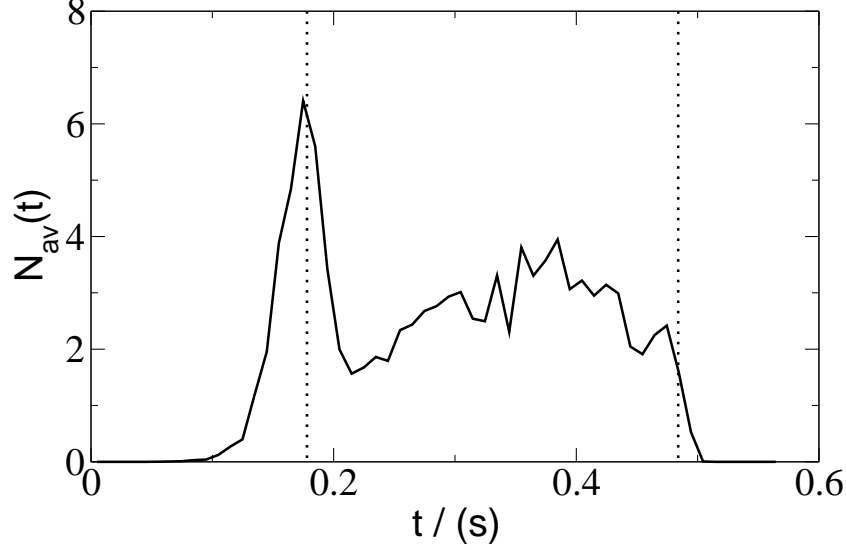


FIG. 11. Spill of the extraction of an Ar^{18+} beam at beam energy $E = 500$ MeV/u bunched with rf fields of the voltage $V_{\text{rf}} = 70$ kV and the harmonic number $h = 100$ obtained by particle tracking. The horizontal tune is moved from $Q_{x,i} = 4.326$ to $Q_{x,f} = 4.334$. Two synchrotron-betatron resonances are crossed which are marked by the dotted vertical lines.

A significant reduction of the influence of the synchro-betatron resonance crossing occurs for reduced rf voltage which is demonstrated in the second step. Figure 12 shows a spill obtained in a simulation, where the rf voltage is reduced to $V_{\text{rf}} = 5$ kV and the horizontal tune interval is changed to $(Q_{x,i}, Q_{x,f}) = (4.329, 4.334)$. All other quantities are preserved from the previous example. Hence, the synchrotron tune is $Q_s = 0.0041$ and three times the horizontal tune interval is $3 \cdot (Q_{x,f} - Q_{x,i}) = 0.015$ such that four resonances are crossed, where the last is the horizontal third integer resonance. The figure shows that the maximum extraction rate occurs between crossing the second and the third crossed resonance. That is a sign that both these resonances are smeared out because they are closer to each other than for $V_{\text{rf}} = 70$ kV and because the synchrotron tune varies with the synchrotron amplitude.

However, goal of the planned installation of the high harmonic rf cavity is the reduction of spill micro structures. Figure 13 shows the time dependent duty factors obtained in simulations for rf fields with voltages $V_{\text{rf}} = 5$ kV and $V_{\text{rf}} = 70$ kV and the harmonic number $h = 100$ compared with that for extraction of unbunched beam. The duty factors found for both rf voltages are at the beginning of the extraction time interval higher than that obtained than that obtained for unbunched beam. The duty factor reduction towards the

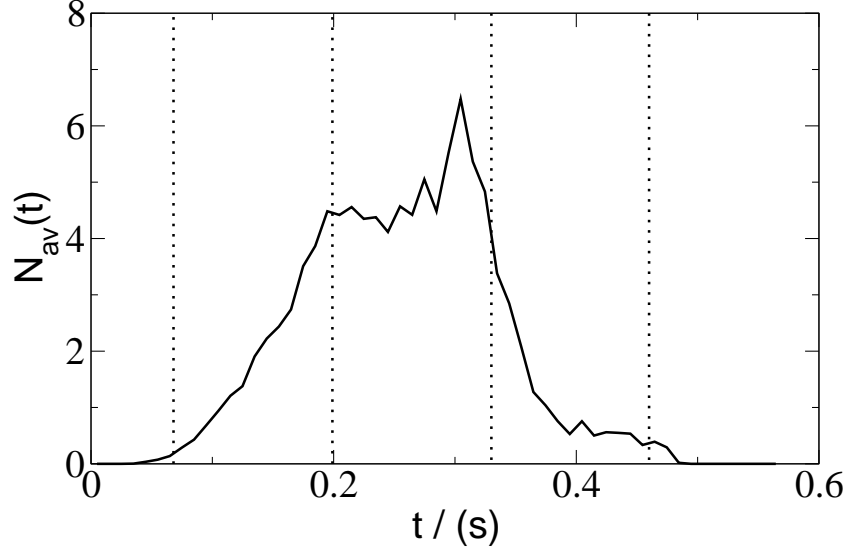


FIG. 12. Spill of the extraction of an Ar^{18+} beam at beam energy $E = 500$ MeV/u bunched with rf fields of the voltage $V_{\text{rf}} = 5$ kV and the harmonic number $h = 100$ obtained by particle tracking. The horizontal tune is moved from $Q_{x,i} = 4.329$ to $Q_{x,f} = 4.334$. The dotted vertical lines denote the instants when synchro-betatron resonances are crossed, the dashed vertical line at $t = 0.048$ s denotes the ending of the rf voltage ramp, and the dashed line at $t = 0.38$ s denotes the crossing of the third integer resonance.

end of the spill found for $V_{\text{rf}} = 5$ kV is, basically, caused by the reduction of the extraction rate which is denoted by the simultaneous reduction of the Poisson duty factor and which can be seen in Figure 12. In contrast to that, the Poisson duty factor found for $V_{\text{rf}} = 70$ kV remains large to the end of the spill and no reduction of the spill at the half extraction time is visible in Figure 11. Hence, that duty factor reduction arises from an increase of the micro spill structure level. These results indicate that an improvement of the spill quality on micro structure level for the rf frequency increased by an order of magnitude is possible, where the spill micro structure mitigation is more efficient when applying a lower rf voltage.

VII. SUMMARY

Bunched beam extraction is a known technique for mitigating the formation of spill micro structures which arise from ripples in the quadrupole magnets of ring accelerators. The quadrupole ripples cause tune ripples and, thereby, a modulation of the size of the stable

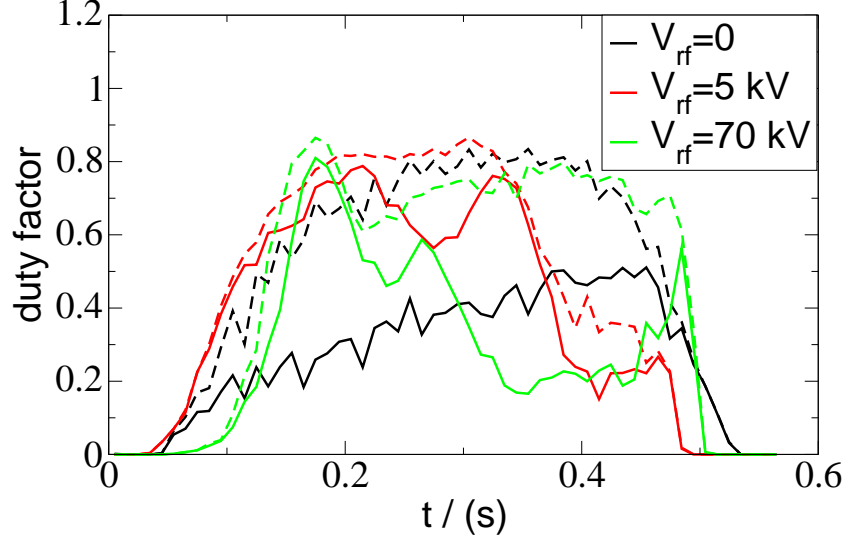


FIG. 13. Duty factors which correspond to the spills in Figures 11 and 12 compared to that obtained with $V_{\text{rf}} = 0$, i.e. without bunching. The dashed curves represent the Poisson duty factors.

phase space area. The resulting structures imprinted on the flow of particles across the edge of the stable phase space area are reduced by synchrotron motion because it decreases the duration of stay of particles near the oscillating separatrices.

We investigated the validity of spill micro structure improvement by bunched beam extraction for larger synchrotron tunes. That was primarily motivated by the plan to install an rf cavity with an rf frequency of $f_{\text{rf}} = 80$ MHz in the GSI heavy ion synchrotron SIS18 which is approximately 20 times the rf frequency of the present cavity.

We found spill improvement only up to an optimum synchrotron tune and diminution of the spill quality for increasing synchrotron tune beyond the optimum. The latter arises from the recapture of particles due to the synchrotron motion. That recapture reduces the transit time of the particles, where average and spread of the transit times are more reduced for a higher synchrotron tune. Therefore, the spill quality defined by micro structures becomes worse at higher cavity voltages.

In addition, **fast** synchrotron motion is found in simulations and spill measurement to cause the formation of macroscopic spill structures of duration ~ 100 ms. Crossing synchro-betatron resonances during the tune sweep could be identified as the source. The structures are better visible for a higher synchrotron tune because the distance between the resonances

is proportional to the synchrotron tune. Consequently, the structures are closer to each other and overlap for lower synchrotron tune such that they are smeared out. Hence, inhibiting the formation of macroscopic structures low can be achieved by setting the rf voltage as low as possible. Further, it was shown that the formation of the macroscopic structures can be reduced by increasing the momentum width or the transverse emittance of the direction used for the extraction, where the latter has a **stronger** impact.

Generally, the formation of macroscopic spill structures as well as the diminution of spill quality mark, in principle, a limitation to the possibility to mitigate spill micro structures by increasing the synchrotron tune in order to reduce the duration of stay of particles near the separatrix.

-
- [1] C. Krantz, T. Fischer, B. Kröck, U. Scheeler, A. Weber, M. Witt, and Th. Haberer, “Slow extraction techniques at the Marburg ion-beam therapy centre”, Contrib. TUPAL036 to the IPAC 2018, Vancouver, BC, Canada, 2018.
 - [2] D. Naito, Y. Kurimoto, R. Muto, T. Kimura, K. Okamura, T. Shimogawa, and M. Tomizawa, “Real-time correction of betatron tune ripples on slowly extracted beam”, Phys. Rev. Accelerators and Beams **22**, 072802 (2019).
 - [3] Y. Kobayashi and H. Takahashi, “Improvement of the emittance in the resonant beam ejection”, Proc. Vth Int. Conf. on High Energy Acc., p. 347, (1967).
 - [4] W. Hardt, “Ultraslow extraction of LEAR”, PS/DL/LEAR Note 81-6, $\bar{p}p$ LEAR Note 98, CERN, 1981.
 - [5] R Singh, P Forck, P Boutachkov, S Sorge and H Welker “Slow Extraction Spill Characterization From Micro to Milli-Second Scale” 2018 *J. Phys.: Conf. Series* **1067** 072002
 - [6] R. Singh, P. Forck, and S. Sorge, “Reducing Fluctuations in Slow-Extraction Beam Spill Using Transit-Time-Dependent Tune Modulation”, Phys. Rev. Applied **13**, 044076 (2020).
 - [7] S Sorge, P Forck and R Singh “Measurements and Simulations of the Spill Quality of Slowly Extracted Beams from the SIS-18 Synchrotron” 2018 *J. Phys.: Conf. Series* **1067** 052003
 - [8] L. Badano, M. Benedikt, P. J. Bryant, M. Crescenti, P. Holy, A. Maier, M. Pullia, and S. Rossi, “Proton-ion medical machine study (PIMMS) part I”, CERN/PS/ 99-010 (DI), Geneva (1999).

- [9] S. Y. Lee, “Accelerator Physics” Second Edition, World Scientific Publishing Co. Pte. Ltd.
- [10] B. Franczak, “SIS Parameter List”, GSI-SIS-TN / 87-13, GSI, Darmstadt, 1987.
- [11] T. Milosic, R. Singh, P. Forck, “Sub-ns single-particle spill characterization for slow extraction”, Contrib. 28 to the 10th Int. Beam. Instrum. Conf., Pohang, Rep. of Korea, 2021.
- [12] J. Pietraszko, “Slow extraction - input from HADES at SIS18”, Presentation during HIC4FAIR Workshop, Darmstadt, Germany, February 2016,
See <https://indico.gsi.de/event/4570>.
- [13] J. Pietraszko, “The HADES/CBM physics case requirements”, Presentation during the Slow Extraction Workshop, Darmstadt, Germany, 2016,
See <https://indico.gsi.de/event/4496>
- [14] P. Schmid, “Planned measures for improving the SIS18 spill quality”, Slow Extraction Workshop, CERN, Geneva, Switzerland, 2017,
see <https://indico.cern.ch/event/639766>
- [15] A. Piwinski, “Synchro-betatron resonances”, CERN, Geneva, Switzerland (1996).